

Lorentz Institute for Theoretical Physics  
Leiden University

Master's Thesis

# **Counting statistics of coherent population trapping in quantum dots\***

Christoph Waldemar Groth

April 2007

Supervised by Prof. Dr. C. W. J. Beenakker

\*The work presented in this thesis has been published in Phys. Rev. B **74**, 125315 (2006).



# Abstract

In this thesis, we theoretically consider a system of three quantum dots. A constant bias voltage is applied via leads connected to the dots. The voltage is assumed to be large, such that tunnelling of electrons between the dots and the leads is irreversible and thus incoherent. Tunneling between the dots themselves is assumed to be reversible.

This setup shows an interesting behavior: an electron can become trapped in a coherent superposition of charge on two of the dots. The trapping is caused by destructive interference of single-electron tunneling between the dots.

In absence of decoherence, one of the electrons passing through the system will become trapped and prevent further flow of current due to Coulomb blockade. In a more realistic case, unavoidable coupling to external charges will cause decoherence which will occasionally disrupt the trapped state thus allowing a certain current to flow.

We calculate the counting statistics of the number of transferred charges, finding a crossover between three parameter regimes featuring sub-Poissonian, Poissonian, and super-Poissonian noise. The physical origin of the system's behavior in these regimes is identified.

For example, in the limit of weak decoherence, on average one electron is transferred through the device for each decoherence event. While some decoherence events temporarily untrap the system causing a cascade of several electrons in quick succession, others immediately cast the system back into the trapped state where it stays for a long time on average. This results in "bunching" of electrons which manifests itself as super-Poissonian statistics.



# Acknowledgements

First of all, I wish to express my gratitude to Prof. Dr. Carlo Beenakker, who supervised and co-authored the research presented in this thesis. His cautious guidance and insightful remarks taught me more about physics than many a course I followed. My thanks also go to Dr. Björn Michaelis for introducing me to the field of mesoscopic transport.

I am indebted to Anton Akhmerov, Luuk Ament, Jens Bardarson, Dr. Thomas Ludwig, Izak Snyman, and other members of Lorentz Institute, who patiently answered my questions and were always open for discussion.

I would like to thank my fellow students with whom I shared the Lorentz Institute student room at various times: Luuk Ament, Bart Clauwens, Jorrit Glastra, Rutger van Haasteren, Jan Willem van de Meent, and Leo van Nierop. We had a very enjoyable time together.

My deep gratitude to many other people and organizations, less directly involved in this thesis, shall remain unspecified here. Thank you all.

Christoph Groth, in April 2007



# Contents

<b>1. Introduction</b>	<b>1</b>
<b>2. Noise in mesoscopic systems</b>	<b>3</b>
2.1. Definition of current noise . . . . .	3
2.2. Full counting statistics . . . . .	4
2.3. Full counting statistics from Lindblad master equation . . . . .	5
2.4. Example: transport through a single quantum dot . . . . .	9
<b>3. Device</b>	<b>13</b>
3.1. Setup and model . . . . .	13
3.2. Modified Lindblad master equation . . . . .	14
<b>4. Solution and results</b>	<b>17</b>
4.1. Analytic solution . . . . .	17
4.1.1. Perturbative approach . . . . .	17
4.1.2. Average current . . . . .	18
4.1.3. Fano factor . . . . .	18
4.1.4. Higher cumulants . . . . .	19
4.2. Limits . . . . .	22
4.2.1. Weak decoherence . . . . .	22
4.2.2. Weak dot-reservoir coupling . . . . .	24
4.2.3. Strong decoherence . . . . .	24
4.2.4. Strong dot-reservoir coupling . . . . .	25
<b>A. Quantum dots</b>	<b>27</b>
<b>B. Lindblad master equation</b>	<b>29</b>
<b>C. Quantum Zeno effect</b>	<b>31</b>

## *Contents*

# 1. Introduction

Noise is usually seen as an unwelcome disturbance of a signal. However, noise, that is fluctuations of a measurement in time, can also present a precious source of information not accessible via the time-averaged value of a measurement [2].

Not all kinds of noise are of equal interest. For example thermal noise, also known as Johnson-Nyquist noise, depends only on temperature – information which is usually more easily acquired in a different way. On the other hand, shot noise, that is noise due to the granularity of charge, depends on properties of the underlying transport process. Among other things, it can provide information about the effective unit of transferred charge and correlations between charges.

In the last two decades of the 20th century, progress in microfabrication techniques has incited interest in electronic transport in nanostructures, e.g. quantum dots (see App. A). The typical length scales in such devices are called mesoscopic: they are much larger than the size of an atom, but small enough to allow quantum effects related to wave coherence, e.g. interference.

One of these is coherent population trapping, originally a phenomenon from quantum optics in which an atomic electron is trapped in a coherent superposition of orbital states by laser illumination. It has been recognized as a useful and interesting concept also in the electronic context [24, 6]. In a mesoscopic implementation, proposed by Michaelis *et al.* [18], the trapping occurs when an electron is coherently distributed over two quantum dots, with a phase difference of  $\pi$  between the two components of the wave function. Portions of the electron's wave function leak from the two dots into a third, where they interfere destructively: the electron cannot tunnel into the third dot.

Advances in experimental technique have allowed to measure not only the conductance but also the noise power in mesoscopic devices [7]. Going further, it has recently become possible to measure the *full counting statistics*, i.e. the statistics of the number of transferred charges in a given time interval. The first two moments of the counting statistics give the mean current and the noise power, and higher moments further specify the correlations between the tunneling electrons [5]. Measurement of the full counting statistics of single-electron transport in a quantum dot has been reported very recently [9, 10]. This development provides a motivation to investigate in this thesis the counting statistics of coherent population trapping, going beyond the first moment studied in Ref. [18].

In Chap. 2, the concepts of noise and full counting statistics are defined. The method to obtain full counting statistics (due to Bagrets and Nazarov[1], and to Kießlich *et al.*[14]) is derived. As an example, counting statistics of tunneling through a single quantum dot is calculated. Chapter 3 specifies the device which implements coherent population trapping and its theoretical description. In Chap. 4 the full counting statis-

## *1. Introduction*

tics for this device is calculated, revealing regimes of sub-Poissonian, Poissonian, and super-Poissonian noise. The physical mechanisms leading to such differing statistics are discussed.

Throughout this thesis we set  $\hbar = 1$ .

## 2. Noise in mesoscopic systems

The objective of this chapter is to provide the tools for Chap. 3 and 4. First, noise power and full counting statistics are introduced. Then the method (due to Bagrets and Nazarov [1], and to Kieflich et al. [14]) to calculate the full counting statistics through a system described by a Lindblad master equation [20, 8] (see App. B) is introduced. Finally, as an example, counting statistics of tunneling through a single quantum dot is calculated.

### 2.1. Definition of current noise

Let us consider a time-dependent current  $I(t)$ . We assume that all external influences are stationary, such that the current's statistics also does not change with time. In practice a stationary process will be also ergodic: an average, denoted by angular brackets  $\langle \dots \rangle$ , can be seen equivalently as an ensemble average or an average over time.

During a time interval of duration  $T$ , the current  $I(t)$  transfers the charge

$$Q(T) = \int_0^T dt I(t). \quad (2.1)$$

The spectral noise power density is defined as the Fourier transform<sup>1</sup>

$$S(\omega) = 2 \int_{-\infty}^{\infty} d\tau e^{-i\omega\tau} C_{II}(\tau) \quad (2.2)$$

of the current-current autocorrelation function

$$C_{II}(\tau) = \langle \delta I(\tau + t) \delta I(t) \rangle = \langle I(\tau + t) I(t) - \langle I \rangle^2 \rangle, \quad (2.3)$$

where  $\delta I(t) = I(t) - \langle I \rangle$ . The autocorrelation function does not depend on the amount of global time shift  $t$ .

Now, we will show that the zero-frequency noise

$$S(0) = 2 \int_{-\infty}^{\infty} d\tau C_{II}(\tau) \quad (2.4)$$

---

<sup>1</sup>Other definitions of noise, e.g. in Quantum optics, leave out the factor of 2.

## 2. Noise in mesoscopic systems

is equal to the variance of the transferred charge per time:

$$S(0) = \lim_{T \rightarrow \infty} 2 \int_{-T}^T d\tau C_{II}(\tau) \quad (2.5a)$$

$$= \lim_{T \rightarrow \infty} \frac{2}{T} \int_0^T d\tau' \int_{-\tau'}^{T-\tau'} d\tau C_{II}(\tau) \quad (2.5b)$$

$$= \lim_{T \rightarrow \infty} \frac{2}{T} \int_0^T d\tau' \int_0^T d\tau C_{II}(\tau - \tau') \quad (2.5c)$$

$$= \lim_{T \rightarrow \infty} \frac{2}{T} \int_0^T d\tau' \int_0^T d\tau \langle I(\tau)I(\tau') - \langle I \rangle^2 \rangle \quad (2.5d)$$

$$= \lim_{T \rightarrow \infty} \frac{2}{T} \left\langle \int_0^T d\tau' \int_0^T d\tau [I(\tau)I(\tau') - \langle I \rangle^2] \right\rangle \quad (2.5e)$$

$$= \lim_{T \rightarrow \infty} \frac{2}{T} \langle Q^2(T) - \langle Q(T) \rangle^2 \rangle. \quad (2.5f)$$

We can carry out the step leading to Expression (2.5b) because the autocorrelation function  $C_{II}(\tau)$  is peaked around  $\tau = 0$ . In Expression (2.5c) we use Eq. (2.3), shifting  $\tau'$  into the second factor.

### 2.2. Full counting statistics

The full counting statistics  $P(n)$  of a transport process is the statistics of the number of charges transferred within a time interval of length  $t$ . Its raw moments  $\langle n^k \rangle$  are given by

$$\langle n^k \rangle = \sum_{n=0}^{\infty} P(n)n^k. \quad (2.6)$$

As one is interested in stationary properties, one chooses for  $t$  a time much longer than all characteristic times of the system responsible for the process, so that any non-stationary initial behavior becomes negligible. Full counting statistics contains information about all possible correlations and moments of charge transfer. For example, mean current is given by the mean number of transferred charges

$$\langle I \rangle = e \frac{\langle n \rangle}{t}, \quad (2.7)$$

$e$  being the unit of elementary charge. According to Eq. (2.5) zero-frequency-noise is given by the variance of transferred charge,

$$S(0) = 2e^2 \frac{\langle n^2 \rangle - \langle n \rangle^2}{t}. \quad (2.8)$$

### 2.3. Full counting statistics from Lindblad master equation

Equivalently, the cumulants  $C_k$  contain all information about the probability distribution  $P(n)$ . These are defined in terms of the cumulant generating function  $F(\chi)$ ,

$$e^{-F(\chi)} = \sum_{n=0}^{\infty} P(n)e^{in\chi}, \quad (2.9)$$

as

$$C_k = -(-i\partial_\chi)^k F(\chi)|_{\chi=0}. \quad (2.10)$$

$C_1$ ,  $C_2$ ,  $C_3$ , and  $C_4$  are, respectively, the mean, variance, asymmetry (“skewness”), and kurtosis (“sharpness”) of  $P(n)$ . Subsequent cumulants contain additional information about the probability distribution. We obtain the average current  $\langle I \rangle = eC_1/t$ , and the zero-frequency noise  $S(0) = 2e^2C_2/t$ .

The dimensionless quantity  $\alpha = C_2/C_1$ , called Fano factor, is a measure of electron-electron correlations. For independent electrons the current fluctuations form a Poisson process. All cumulants are equal, and we have  $\alpha = 1$ . A Fano factor smaller than 1 indicates negative correlations between electrons (anti-bunching)<sup>2</sup>. Conversely, positive electron-electron correlations (bunching), lead to an increase of noise signaled by a Fano factor larger than one. Depending on the Fano factor being smaller, equal, or greater than unity, one speaks of a sub-Poissonian, Poissonian, or super-Poissonian process, respectively.

One can also define “generalized Fano factors”  $C_3/C_1$ ,  $C_4/C_1$ ,  $\dots$ , that quantify correlations of higher order. As we will see, for the systems considered in this thesis, these quantities tend to behave similarly to the Fano factor. Consequently, we will mainly restrict ourselves to an analysis of the first two cumulants.

### 2.3. Full counting statistics from Lindblad master equation

The time evolution of an open quantum system interacting with a memory-less (i.e. Markovian) environment can be expressed as a *Lindblad master equation* (see App. B). In this section it will be shown how to obtain the full counting statistics of a transport process by modifying this scheme. In short this works as follows: We write the Lindblad equation as  $dv/dt = Mv$ , collecting the elements of the density matrix in a vector  $v$ . We multiply one or a few distinguished elements of  $M$  by *counting factors*  $e^{i\chi}$  (or integer powers thereof). The cumulant generating function is then given by the eigenvalue of the modified  $M$  whose real part is closest to zero.

The analysis leading to Eq. (2.18) is due to Izak Snyman of Lorentz Institute.

Consider a density matrix  $\rho$  describing the state of an open quantum system, and its Lindblad form equation of motion (B.1):

$$\frac{d\rho}{dt} = -i[H, \rho(t)] + \sum_{\mu} \left( L_{\mu}\rho(t)L_{\mu}^{\dagger} - \frac{1}{2}L_{\mu}^{\dagger}L_{\mu}\rho(t) - \frac{1}{2}\rho(t)L_{\mu}^{\dagger}L_{\mu} \right).$$

---

<sup>2</sup>In the case of extreme anti-bunching, subsequent electrons follow each other after equal time intervals and the Fano factor vanishes.

## 2. Noise in mesoscopic systems

This can be expressed as

$$\frac{d\rho}{dt} = \left(-iH - \frac{\Lambda}{2}\right) \rho(t) + \rho(t) \left(iH - \frac{\Lambda}{2}\right) + \sum_{\mu} L_{\mu} \rho(t) L_{\mu}^{\dagger}, \quad (2.11)$$

where  $\Lambda = \sum_{\mu} L_{\mu}^{\dagger} L_{\mu}$ . The quantum jump operators  $L_{\mu}$  describe transitions in the system induced by the environment.  $H$  is the Hamiltonian of the system in absence of coupling to the environment. Let us transform  $\rho(t)$  to the interaction picture:

$$\rho_I(t) := e^{(iH + \frac{\Lambda}{2})t} \rho(t) e^{(-iH + \frac{\Lambda}{2})t}, \quad (2.12a)$$

$$L_{\mu}(t) := e^{(iH + \frac{\Lambda}{2})t} L_{\mu} e^{(-iH - \frac{\Lambda}{2})t}. \quad (2.12b)$$

Note the different sign in front of  $\frac{\Lambda}{2}$  in the second exponential of both formula. Taking the time derivative of Eq. (2.12a) and using Eq. (2.11), one obtains the equation of motion for  $\rho_I$ :

$$\frac{d\rho_I}{dt} = \sum_{\mu} L_{\mu}(t) \rho_I(t) L_{\mu}^{\dagger}(t). \quad (2.13)$$

This can be converted to an integral equation, subject to the boundary condition  $\rho_I(0) = \rho_0$ , and solved iteratively making use of the rule

$$\rho_I^{(n+1)}(t) = \rho_0 + \sum_{\mu} \int_0^t d\tau L_{\mu}(\tau) \rho_I^{(n)}(\tau) L_{\mu}^{\dagger}(\tau) \quad (2.14)$$

to get

$$\begin{aligned} \rho_I(t) &= \rho_I^{(\infty)}(t) \\ &= \rho_0 + \sum_{k=1}^{\infty} \sum_{\mu_1, \dots, \mu_k} \int_0^t dt_1 \int_0^{t_1} dt_2 \dots \int_0^{t_{k-1}} dt_k L_{\mu_1}(t_1) \dots \\ &\quad \dots L_{\mu_k}(t_k) \rho_0 L_{\mu_k}^{\dagger}(t_k) \dots L_{\mu_1}^{\dagger}(t_1). \end{aligned} \quad (2.15)$$

Consider an initial density matrix  $\rho_0 = |\psi\rangle\langle\psi|$ , and investigate the probability

$$\langle\phi|\rho(t)|\phi\rangle = \langle\phi|e^{(-iH - \frac{\Lambda}{2})t} \rho_I(t) e^{(iH - \frac{\Lambda}{2})t} |\phi\rangle \quad (2.16)$$

to find the system in state  $|\phi\rangle$  at time  $t$ . An arbitrary  $k$ 'th order term of the expansion derived by inserting Eq. (2.15) into Eq. (2.16) has the form

$$\begin{aligned} &\left| \langle\phi| e^{(-iH - \frac{\Lambda}{2})(t-t_1)} L_{\mu_1} e^{(-iH - \frac{\Lambda}{2})(t_1-t_2)} L_{\mu_2} \dots \right. \\ &\quad \left. \dots e^{(-iH - \frac{\Lambda}{2})(t_{k-1}-t_k)} L_{\mu_k} e^{(-iH - \frac{\Lambda}{2})t_k} |\psi\rangle \right|^2 dt_1 dt_2 \dots dt_k, \end{aligned} \quad (2.17)$$

with  $t_1 > t_2 > \dots > t_k > 0$ . It is natural to interpret this as the probability for the following sequence of events: From time 0 to time  $t_k$  the system evolves with  $H - i\Lambda/2$

### 2.3. Full counting statistics from Lindblad master equation

as generator of time-translation.<sup>3</sup> At time  $t_k$  the environment induces the transition described by the operator  $L_{\mu_k}$ . Between times  $t_k$  and  $t_{k-1}$  the system again evolves subject to  $H - i\Lambda/2$  up to  $t$ , and ends up in the state  $|\phi\rangle$ . The total probability of finding the system in the state  $|\phi\rangle$  is the sum over the probabilities (as opposed to the square of the modulus of the sum of amplitudes) of all such sequences of events. The  $k$ 'th order term in Eq. (2.15) represents the sum over all sequences of events containing  $k$  transitions induced by the environment. We see that quantities depending only on the numbers of events are classical stochastic variables.

To be more specific, let us consider an electronic transport problem: A system is connected to a left and a right lead. The coherent time evolution of the system is governed by a Hamiltonian  $H$ . Interactions with the leads and the environment are modelled by quantum jump operators  $L_\mu$ . For each operator we denote the number of electrons transferred by a single event from the system into the right lead (or, equivalently<sup>4</sup>, from the left lead into the system) as  $\sigma_\mu$ . For example,  $\sigma_\mu$  will have the value  $-1$  for an event transferring a single electron from the right lead into the system. If an event is not related to transport between the system and the right lead,  $\sigma_\mu$  will be zero.

In order to obtain the counting statistics, we now introduce the counting field  $\chi$ . The counting field  $\chi$  and the number of transferred charges  $n$  are conjugate variables connected by the Fourier transform (2.9). We replace the jump operators  $L_\mu$  in the amplitude  $\langle\phi|\dots|\psi\rangle$  of term (2.17) by  $e^{i\chi\sigma_\mu}L_\mu$  without replacing the adjoint operators  $L_\mu^\dagger$  in the amplitude  $\langle\psi|\dots|\phi\rangle$ . As the result we get the old value, being the probability of the sequence of events  $\{\mu_k, t_k\}$ , multiplied by a factor  $e^{i\chi n(\{\mu_k\})}$ , where  $n(\{\mu_k\}) = \sum_k \sigma_{\mu_k}$  is the number of electrons effectively transferred into the right lead by that sequence of events. But Eqs. (2.15) and (2.17) with the modified  $L_\mu$  can be found as solution of the modified Lindblad equation

$$\frac{d\rho_\chi}{dt} = \left(-iH - \frac{\Lambda}{2}\right)\rho_\chi(t) + \rho_\chi(t)\left(iH - \frac{\Lambda}{2}\right) + \sum_\mu e^{i\chi\sigma_\mu}L_\mu\rho_\chi(t)L_\mu^\dagger. \quad (2.18)$$

Knowledge of  $\rho_\chi(t)$  gives us, by Eq. (2.9), the full counting statistics of the transfer process for the time interval running from 0 to  $t$ :

$$e^{-F(\chi)} = \sum_{n=0}^{\infty} P(n)e^{in\chi} = \langle e^{in\chi} \rangle = \text{Tr}[\rho_\chi(t)]. \quad (2.19)$$

As the final step in obtaining the full counting statistics, let us collect all unique coefficients of the Hermitian matrix  $\rho_\chi$  into a vector  $v_\chi$ . Equation (2.18) obtains the simple

<sup>3</sup>The term  $-i\Lambda/2$  introduces decay. This is necessary in order to ensure proper normalization of  $\rho_t$  at all times. The decay term can also be seen as reducing exponentially with time the probability of coherent evolution as described by  $H$ .

<sup>4</sup>The number of electrons transferred from the left lead into the system and the number of electrons transferred from the system into the right lead are equal up to the amount of electrons that can stay inside the system, which is finite. The difference becomes negligible for the long times  $t$  which will be considered in this analysis.

## 2. Noise in mesoscopic systems

form

$$\frac{dv_\chi}{dt} = M_\chi v_\chi(t), \quad (2.20)$$

where the matrix  $M_\chi$  encodes the couplings between elements of  $v_\chi(t)$  in accordance with Eq. (2.18). The formal solution of Eq. (2.20) can be written as

$$v_\chi(t) = e^{M_\chi t} v_\chi(0). \quad (2.21)$$

Equation (2.19) becomes

$$e^{-F(\chi)} = \sum_{i \in D} [v_\chi(t)]_i, \quad (2.22)$$

where  $(\dots)_i$  denotes the  $i$ 'th element of a vector, and  $D$  is the set of all elements of  $v_\chi$  which were diagonal elements of  $\rho_\chi$ . On our way to a useful expression for  $F(\chi)$ , we plug Eq. (2.21) into Eq. (2.22): and express  $v_\chi(0)$  in terms of eigenvectors  $w_l$  of  $M_\chi$  with eigenvalues  $\lambda_l$ :

$$e^{-F(\chi)} = \sum_{i \in D} \left( e^{M_\chi t} v_\chi(0) \right)_i = \sum_{i \in D} \left( e^{M_\chi t} \sum_l w_l \right)_i = \sum_l \sum_{i \in D} \left( e^{\lambda_l t} w_l \right)_i. \quad (2.23)$$

Defining the constants  $\gamma_l = \sum_{i \in D} [w_l]_i$ , we can write:

$$e^{-F(\chi)} = \sum_l e^{\lambda_l t} \gamma_l. \quad (2.24)$$

The real parts of all eigenvalues  $\lambda_l$  have to be non-positive. Otherwise, for times  $t$  going to infinity, the integral over the squared modulus of  $e^{-F(\chi)}$  would not stay finite, which would be in conflict with the finite norm of  $P(n)$  of which  $e^{-F(\chi)}$  is the Fourier transform.

For the long times  $t$  under consideration, only the term of Eq. (2.24) contributes whose eigenvalue  $\lambda_l$  has the smallest absolute real part. Thus we obtain

$$F(\chi) = -\lambda_{\min} t - \ln \gamma_{\min},$$

where  $\lambda_{\min}$  denotes the eigenvalue of  $M_\chi$  which vanishes for  $\chi = 0$ , and  $\gamma_{\min}$  is the corresponding constant  $\gamma_l$ . As we are only interested in derivatives of  $F(\chi)$  the constant term  $\ln \gamma_{\min}$  plays no role and can be omitted:

$$F(\chi) = -\lambda_{\min} t \quad (2.25)$$

As a final remark, we see from Eq. (2.9) that due to conservation of probability,  $F(0)$  and thus also  $\lambda_{\min}|_{\chi=0}$  vanish for all times  $t$ .

## 2.4. Example: transport through a single quantum dot

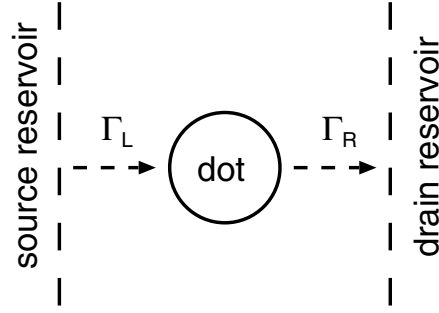


Figure 2.1.: A single quantum dot connected to a source and a drain reservoir. Irreversible transitions (rates  $\Gamma_L$  and  $\Gamma_R$ ) are indicated by arrows.

### 2.4. Example: transport through a single quantum dot

As a simple example we calculate the full counting statistics of transport through a single quantum dot connected to two reservoirs (leads), as depicted schematically in Fig. 2.1. In the limit of large bias voltage, which we consider here, electron tunneling from the source reservoir into the dot and from the dot into the drain reservoir is irreversible. We assume that a single level in the dot lies within range of the bias voltage, and that, because of Coulomb blockade, at most a single electron can occupy the dot. The set of basis states, therefore, consists of the states  $|0\rangle$ , and  $|1\rangle$ , in which the dot is, respectively, empty, and occupied by one electron.

The time evolution of the system's density matrix  $\rho$  is given by the Lindblad master equation (B.1). As there is no internal dynamics, the Hamiltonian  $H$  vanishes. The quantum jump operators

$$L_L = \sqrt{\Gamma_L} |1\rangle \langle 0|, \quad L_R = \sqrt{\Gamma_R} |0\rangle \langle 1|$$

model irreversible tunneling into and out of the dot, with the rates  $\Gamma_L$  and  $\Gamma_R$ , respectively.

Having specified the evolution of the system in terms of a Lindblad master equation, we can proceed to calculate the full counting statistics along the lines of section 2.3. Let us count the electrons moving from the system into the right lead, i.e.  $\sigma_L = 0$ , and  $\sigma_R = 1$ . We have:

$$\Lambda = \sum_{\mu} L_{\mu}^{\dagger} L_{\mu} = \Gamma_L |0\rangle \langle 0| + \Gamma_R |1\rangle \langle 1|. \quad (2.26)$$

Now we can write down the modified Lindblad master equation (2.18):

$$\begin{aligned} \frac{d\rho_X}{dt} &= - \frac{\Gamma_L |0\rangle \langle 0| + \Gamma_R |1\rangle \langle 1|}{2} \rho_X - \rho_X \frac{\Gamma_L |0\rangle \langle 0| + \Gamma_R |1\rangle \langle 1|}{2} \\ &\quad + \Gamma_L |1\rangle \langle 0| \rho_X |0\rangle \langle 1| + e^{iX} \Gamma_R |0\rangle \langle 1| \rho_X |1\rangle \langle 0| \\ &= \begin{pmatrix} e^{iX} \Gamma_R (\rho_X)_{11} - \Gamma_L (\rho_X)_{00} & -\frac{1}{2} (\Gamma_L + \Gamma_R) (\rho_X)_{01} \\ -\frac{1}{2} (\Gamma_L + \Gamma_R) (\rho_X)_{10} & \Gamma_L (\rho_X)_{00} - \Gamma_R (\rho_X)_{11} \end{pmatrix}. \end{aligned} \quad (2.27)$$

## 2. Noise in mesoscopic systems

We see that if we choose a diagonal initial state  $\rho_0$ , the non-diagonal elements of  $\rho_\chi$  will remain zero. Therefore, it is sufficient to collect the diagonal elements of  $\rho_\chi$  into  $v_\chi$ :

$$v_\chi = \begin{pmatrix} (\rho_\chi)_{00} \\ (\rho_\chi)_{11} \end{pmatrix}. \quad (2.28)$$

The time evolution of  $v_\chi$  follows from Eq. (2.27) as

$$\frac{d\rho_\chi}{dt} = M_\chi v_\chi, \quad M_\chi = \begin{pmatrix} -\Gamma_L & e^{i\chi}\Gamma_R \\ \Gamma_L & -\Gamma_R \end{pmatrix}. \quad (2.29)$$

$M_\chi$  has two eigenvalues,

$$\lambda_{0,1} = \frac{-\Gamma_L - \Gamma_R \pm \sqrt{(\Gamma_L - \Gamma_R)^2 + 4e^{i\chi}\Gamma_L\Gamma_R}}{2}, \quad (2.30)$$

of which the one with a plus-sign in front of the square root has a real value closer to zero. Thus, by Eq. (2.25), we obtain the cumulant generating function

$$F(\chi) = -\lambda_{\min} t = t \frac{\Gamma_L + \Gamma_R - \sqrt{(\Gamma_L - \Gamma_R)^2 + 4e^{i\chi}\Gamma_L\Gamma_R}}{2}. \quad (2.31)$$

The final step is to evaluate the derivatives of  $F(\chi)$  at  $\chi = 0$ . This yields the cumulants according to Eq. (2.10):

$$C_1 = t \frac{\Gamma_L \Gamma_R}{\Gamma_L + \Gamma_R}, \quad C_2 = t \frac{\Gamma_L \Gamma_R (\Gamma_L^2 + \Gamma_R^2)}{(\Gamma_L + \Gamma_R)^3}. \quad (2.32)$$

(We do not display the expressions for subsequent cumulants, because they get increasingly lengthy and decreasingly informative. See Fig. 2.2, though.) In analogy to the current flowing through two resistors with resistances  $\Gamma_L^{-1}$  and  $\Gamma_R^{-1}$  in series, we find the mean current to be

$$\langle I \rangle = e \frac{C_1}{t} = e \frac{\Gamma_L \Gamma_R}{\Gamma_L + \Gamma_R}, \quad (2.33)$$

For the Fano factor we obtain

$$\alpha = \frac{C_2}{C_1} = \frac{\Gamma_L^2 + \Gamma_R^2}{(\Gamma_L + \Gamma_R)^2}. \quad (2.34)$$

Figure 2.2 is a plot of normalized average current  $\langle I \rangle / e\Gamma_R = C_1/\Gamma_R t$ , Fano factor, and the ‘‘generalized Fano factors’’  $C_3/C_1$  and  $C_4/C_1$  as a function of the ratio of tunnel rates  $\Gamma_L/\Gamma_R$ . We see that Poissonian statistics is approached for strongly asymmetric coupling, with sub-Poissonian statistics in between. Higher order cumulants behave similarly to the Fano factor. The mechanism behind the anti-bunching observed for  $\Gamma_L \simeq \Gamma_R$  is easily explained: as the dot can hold only one electron (Coulomb blockade), it takes some time to fill the vacant dot after an electron has left. This queuing effect breaks down when the rates differ vastly, leading to Poisson statistics.

It will be interesting to note for the analysis done in Section 4.2.2, that in the special case  $\Gamma_L \rightarrow 2\Gamma, \Gamma_R \rightarrow \Gamma/3$  we get:

$$\langle I \rangle = \frac{2}{7}e, \quad \alpha = \frac{37}{49}. \quad (2.35)$$

## 2.4. Example: transport through a single quantum dot

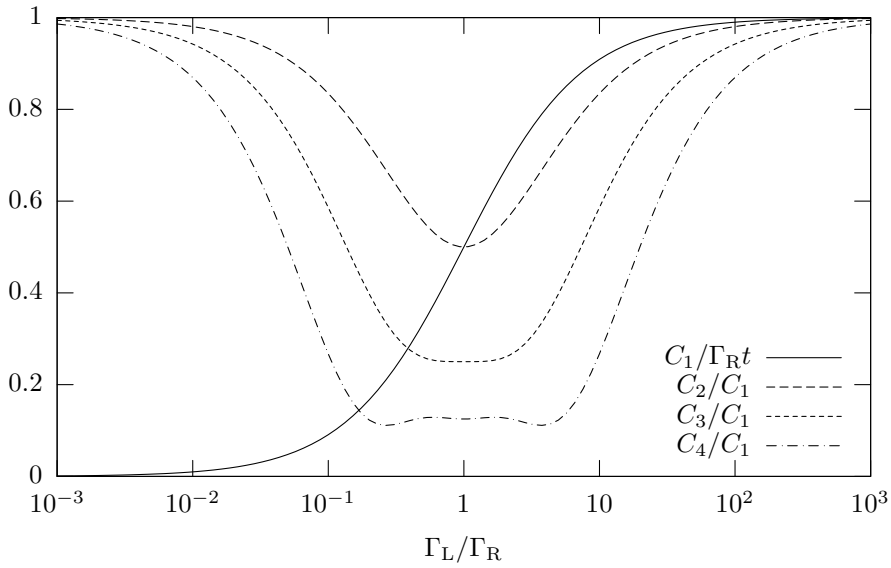


Figure 2.2.: Four dimensionless quantities derived from the first four cumulants of transport in a single one-level quantum dot, plotted as a function of the ratio of tunnel rates  $\Gamma_L/\Gamma_R$ .  $C_1/\Gamma_R t$  is the normalized average current,  $C_2/C_1$  the Fano factor.  $C_3/C_1$  and  $C_4/C_1$  are “generalized Fano factors” quantifying, respectively, the “skewness” and the “sharpness” of the probability distribution  $P(n)$  of the number of transferred charges.

## 2. *Noise in mesoscopic systems*

## 3. Device

In this chapter, an all-electronic implementation of coherent population trapping in quantum dots (proposed by Michaelis *et al.* [18]) is introduced. A modified Lindblad master equation (see Sec. 2.3) is derived which will allow to calculate the full counting statistics. For a short introduction to quantum dots see App. A.

### 3.1. Setup and model

The system is depicted schematically in Fig. 3.1. It consists of three tunnel-coupled quantum dots connected to two electron reservoirs (leads). In the limit of large bias voltage, which we consider here, electron tunneling from the source reservoir into the dots and from the dots into the drain reservoir is irreversible. We assume that a single level in each dot lies within range of the bias voltage. We also assume that due to Coulomb blockade there can be at most one electron in total in the three dots. The basis states, therefore, consist of the state  $|0\rangle$  in which all dots are empty, and the states  $|A\rangle$ ,  $|B\rangle$ , and  $|C\rangle$  in which a single electron occupies one of the dots.

The time evolution of the density matrix  $\rho$  for the system is given by the Lindblad-type master equation,

$$\frac{d\rho}{dt} = -i[H, \rho] + \sum_{\mu=A,B,C,\phi_A,\phi_B,\phi_C} (L_\mu \rho L_\mu^\dagger - \frac{1}{2} L_\mu^\dagger L_\mu \rho - \frac{1}{2} \rho L_\mu^\dagger L_\mu), \quad (3.1)$$

which is an instance of Eq. (B.1).

The Hamiltonian

$$H = T|C\rangle\langle A| + T|C\rangle\langle B| + \text{H.c.} \quad (3.2)$$

is responsible for reversible tunneling between the dots, with tunnel rate  $T$ , which we assume to be positive<sup>1</sup>. For simplicity, we assume that the three energy levels in dots A, B, and C are degenerate and that the two tunnel rates from A to C and from B to C are the same.

The quantum jump operators

$$L_A = \sqrt{\Gamma}|A\rangle\langle 0|, \quad L_B = \sqrt{\Gamma}|B\rangle\langle 0|, \quad L_C = \sqrt{\Gamma}|0\rangle\langle C|, \quad (3.3)$$

model irreversible tunneling out of and into the reservoirs, with a rate  $\Gamma$  (which we again take the same for each dot). Finally, the quantum jump operators

$$L_{\phi_X} = \sqrt{\Gamma_\phi}|X\rangle\langle X|, \quad X = A, B, C, \quad (3.4)$$

---

<sup>1</sup>When  $T$  is an arbitrary complex number, we can make it positive by absorbing its phase into  $|C\rangle$ .

### 3. Device

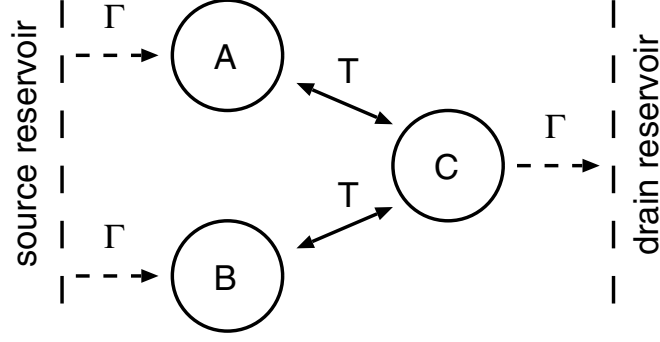


Figure 3.1.: Three quantum dots connected to a source and a drain reservoir. Reversible transitions (rate  $T$ ) and irreversible transitions (rate  $\Gamma$ ) are indicated by arrows.

model decoherence due to charge noise with a rate  $\Gamma_\phi$ . It is reasonable to model decoherence in this way by projecting onto the dot-states  $|A\rangle$ ,  $|B\rangle$ , and  $|C\rangle$ , because decoherence is caused by external charges measuring the location of the electron in the system.

As a basis for the the density matrix we use the four states

$$\begin{aligned} |e_1\rangle &= 2^{-1/2}(|A\rangle + |B\rangle), \\ |e_2\rangle &= 2^{-1/2}(|A\rangle - |B\rangle), \\ |e_3\rangle &= |C\rangle, \quad |e_4\rangle = |0\rangle. \end{aligned} \quad (3.5)$$

Now the Hamiltonian can also be written as

$$H = \sqrt{2}T|C\rangle\langle e_1| + \text{H.c.}, \quad (3.6)$$

and we see that  $|e_2\rangle$  is the trapped state.

### 3.2. Modified Lindblad master equation

In order to extract the full counting statistics, we have to modify the Lindblad master equation by introducing counting factors  $e^{ix\sigma_\mu}$  according to the method of Sec. 2.3. We wish to arrive at an instance of Eq. (2.21). The procedure is the same as in the first part of Sec. 2.4.

We are free to choose whether to count incoming or outgoing electrons. To keep things simple, let us count electrons leaving dot C for the right lead. Consequently, the counting factors associated with all jump operators are 1, with the exception of the counting factor of  $L_C$  which is  $e^{ix}$ . The only term in the modified master equation containing a counting factor will be therefore

$$e^{ix}L_C\rho_\chi(t)L_C^\dagger = \Gamma e^{ix}|0\rangle\langle C|\rho_\chi(t)|C\rangle\langle 0|. \quad (3.7)$$

### 3.2. Modified Lindblad master equation

If the initial state is  $|0\rangle\langle 0|$ , most of the coefficients of  $\rho_X$  will remain zero. We collect the five non-zero variables in a vector

$$v_X = \left( (\rho_X)_{11}, (\rho_X)_{22}, (\rho_X)_{33}, (\rho_X)_{44}, \text{Im}(\rho_X)_{13} \right)^T, \quad (3.8)$$

whose time evolution follows from Eq. (2.18) as

$$\frac{dv_X}{dt} = M_X v_X, \quad M_X = \begin{pmatrix} -\Gamma_\phi/2 & \Gamma_\phi/2 & 0 & \Gamma & -2^{3/2}\Upsilon \\ \Gamma_\phi/2 & -\Gamma_\phi/2 & 0 & \Gamma & 0 \\ 0 & 0 & -\Gamma & 0 & 2^{3/2}\Upsilon \\ 0 & 0 & \Gamma e^{iX} & -2\Gamma & 0 \\ 2^{1/2}\Upsilon & 0 & -2^{1/2}\Upsilon & 0 & -\Gamma/2 - \Gamma_\phi \end{pmatrix}. \quad (3.9)$$

The eigenvalue of  $M_X$  whose real part is closest to zero will yield the cumulant generating function.

### 3. *Device*

## 4. Solution and results

In this chapter, mesoscopic transport in the system introduced in Chap. 3 is analyzed. A perturbative approach is employed to obtain the first four cumulants of the statistics of the number of transferred charges. A discussion follows in which parameter regimes characterized by Poissonian, sub-Poissonian, and super-Poissonian noise are identified. In the final section, the behavior of the system at limits typical for the different regimes is examined in detail.

### 4.1. Analytic solution

#### 4.1.1. Perturbative approach

To obtain the cumulant generating function  $F(\chi)$  by Eq. (2.25), we seek the eigenvalue  $\lambda_{\min}$  of  $M_\chi$  (as defined in Eq. (3.9)) whose real part is closest to zero. Unfortunately,  $M_\chi$  is a  $5 \times 5$  matrix with complex coefficients, making a direct calculation impossible. However, setting  $\chi = 0$ , it is possible to find an exact expression for the eigenvector  $w_{\min|\chi=0}$ . This is the stationary solution of the unmodified master equation. As the stationary solution is invariable in time, the corresponding eigenvalue  $\lambda_{\min|\chi=0}$  must vanish.

In the following we will denote the rate matrix  $M_\chi$  by  $M$ , its smallest eigenvalue  $\lambda_{\min}$  by  $\lambda$ , and the corresponding eigenvector  $w_{\min}$  by  $w$ .

To calculate cumulants up to  $C_n$  by Eq. (2.10), it is sufficient to know the cumulant generating function to  $n$ 'th order in  $\chi$ . The wanted eigenvalue  $\lambda$  of the rate matrix  $M$  has the expansion

$$\lambda = \lambda_0 + \lambda_1\chi + \lambda_2\chi^2 + \dots, \quad (4.1)$$

where  $\lambda_0 = \lambda_{\min|\chi=0} = 0$ . We also express the eigenvector  $w$  and the matrix itself in a power series in  $\chi$ :

$$w = w_0 + w_1\chi + w_2\chi^2 + \dots, \quad (4.2)$$

$$M = M_0 + M_1\chi + M_2\chi^2 + \dots. \quad (4.3)$$

Inserting the above expansions into the eigenvalue equation  $M = \lambda w$  yields the following relationships of respective order zero, one, two, and so on:

$$M_0 w_0 = 0, \quad (4.4a)$$

$$M_1 w_0 + M_0 w_1 = \lambda_1 w_0, \quad (4.4b)$$

$$M_2 w_0 + M_1 w_1 + M_0 w_2 = \lambda_2 w_0 + \lambda_1 w_1, \quad (4.4c)$$

⋮

#### 4. Solution and results

The coefficients  $M_k$  are known, while  $w_k$  and  $\lambda_k$  remain to be found by solving these equations sequentially, starting with the known  $w_0 = w_{\min}|_{\chi=0}$ . The cumulants then follow from Eq. (2.10) as

$$C_1 = -it\lambda_1, \quad C_2 = -2t\lambda_2, \quad \dots \quad (4.5)$$

For completeness we provide the exact stationary solution:

$$w_0 = \begin{pmatrix} (\Gamma^2 + 2\Gamma\Gamma_\phi + 8T^2)/2\beta \\ (\Gamma^2 + 2\Gamma\Gamma_\phi + 8T^2\Gamma_\phi + 8T^2\Gamma/\Gamma_\phi)/2\beta \\ 4T^2/\beta \\ 2T^2/\beta \\ \sqrt{2}\Gamma/\beta \end{pmatrix}, \quad (4.6)$$

where

$$\beta = \Gamma^2 + 14T^2 + 2\Gamma\Gamma_\phi(1 + 2T^2/\Gamma_\phi^2).$$

##### 4.1.2. Average current

By following the procedure just outlined we find (in agreement with Ref. [18]) the average current

$$\langle I \rangle = C_1 e = 4eT^2\Gamma/\beta, \quad (4.7)$$

shown in Fig. 4.1. As one might surmise,  $\langle I \rangle$  is equal to the occupation probability of dot C (third component of  $w_0$ , see Eq. (4.6)) multiplied by  $\Gamma$ . The average current reaches its maximum value

$$I_{\max} = \frac{\sqrt{14}T}{7 + 2\sqrt{7}}e \quad (4.8)$$

for  $\Gamma = \sqrt{14}T$  and  $\Gamma_\phi = \sqrt{2}T$ .

##### 4.1.3. Fano factor

Calculating the successive cumulant we obtain the Fano factor

$$\begin{aligned} \alpha &= C_2/C_1 \\ &= \frac{\Gamma^4 + 148T^4 + 2\Gamma\Gamma_\phi(16T^2 + 2\Gamma^2)(1 + 2T^2/\Gamma_\phi^2) + 4\Gamma^2(\Gamma_\phi^2 + 4T^2 + 12T^4/\Gamma_\phi^2)}{\beta^2}. \end{aligned} \quad (4.9)$$

At the point of maximum average current, the Fano factor assumes the slightly sub-Poissonian value  $(127 + 44\sqrt{7})/(154 + 56\sqrt{7}) \simeq 0.806$ .

In Fig. 4.2, the Fano factor is shown as a function of  $\Gamma_\phi/T$  and  $\Gamma/T$ . Additionally, three cuts through Fig. 4.2 at constant  $\Gamma/T$  have been plotted in Fig. 4.3. The plots clearly show three parameter regimes in which the Fano factor assumes a largely constant value. A region of super-Poissonian ( $\alpha > 1$ ) noise appears in the limit of weak decoherence, sub-Poissonian ( $\alpha < 1$ ) noise in the limit of slow dot-reservoir tunneling, and Poissonian

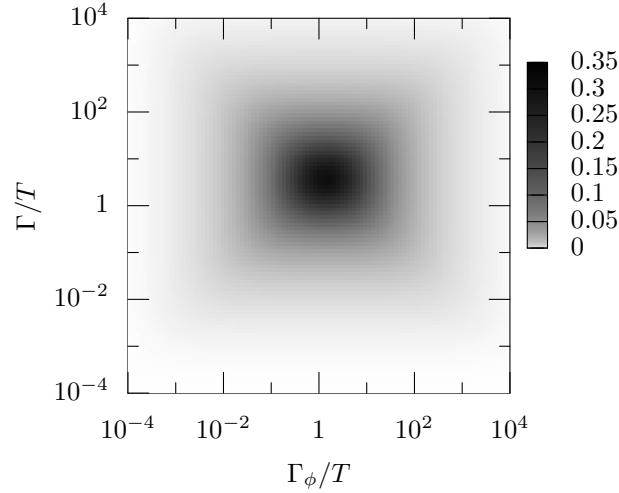


Figure 4.1.: Normalized average current  $\langle\langle I \rangle\rangle / e\Gamma_R = C_1/\Gamma_R t$  as a function of normalized decoherence rate  $\Gamma_\phi/T$  and normalized reservoir-dot tunnel rate  $\Gamma/T$ .

( $\alpha = 1$ ) noise both in the limit of strong decoherence as well as fast dot-reservoir tunneling. Two “rims” in which the Fano factor assumes a low value separate the realm of sub-Poissonian noise from the other two domains. Physical explanations for all four limiting cases will be presented at the end of this chapter. We have no simple physical picture for the appearance of the rims.

#### 4.1.4. Higher cumulants

We have also calculated exact (and very lengthy) expressions for  $C_3$  and  $C_4$ , and could, in principle, continue further. However, as can be seen from Fig. 4.4, showing “generalized Fano factors”  $C_3/C_1$  and  $C_4/C_1$ , no qualitatively new features appear.

#### 4. Solution and results

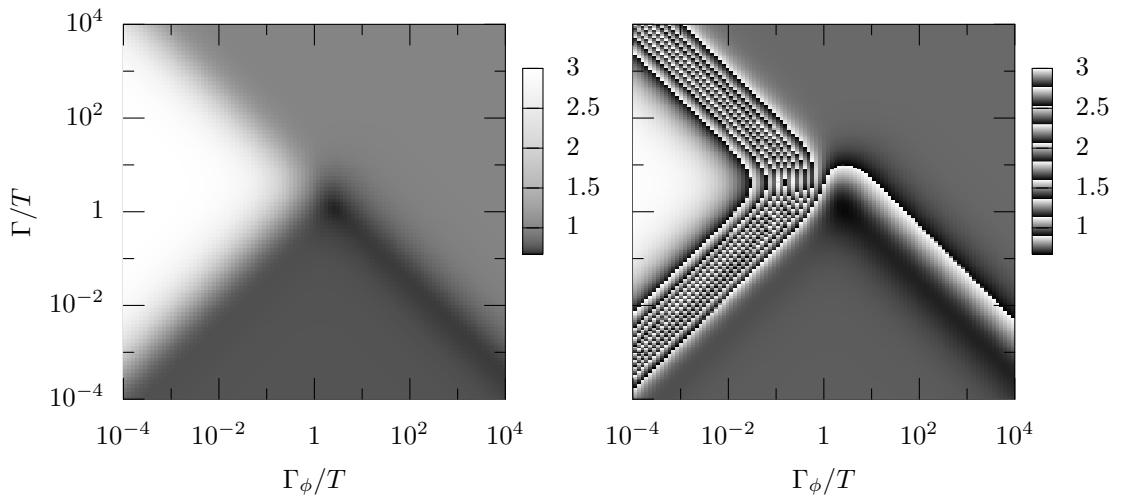


Figure 4.2.: Fano factor  $\alpha$  as a function of normalized decoherence rate  $\Gamma_\phi/T$  and normalized reservoir-dot tunnel rate  $\Gamma/T$ . The gray-scale-scheme used to produce the right plot was chosen to make fine differences in the value of  $\alpha$  visible more easily.

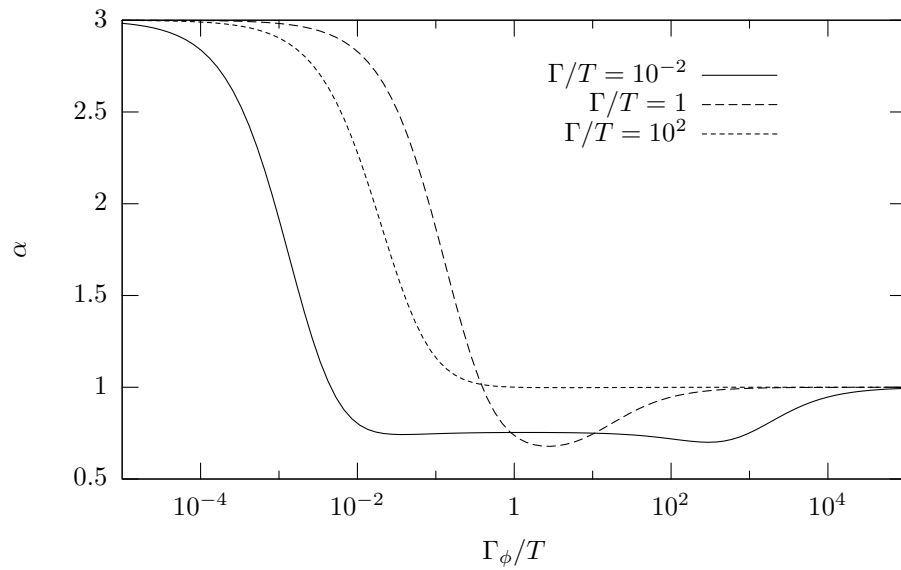


Figure 4.3.: Dependence of Fano factor  $\alpha$  on normalized decoherence rate  $\Gamma_\phi/T$  for three values of  $\Gamma/T$ .

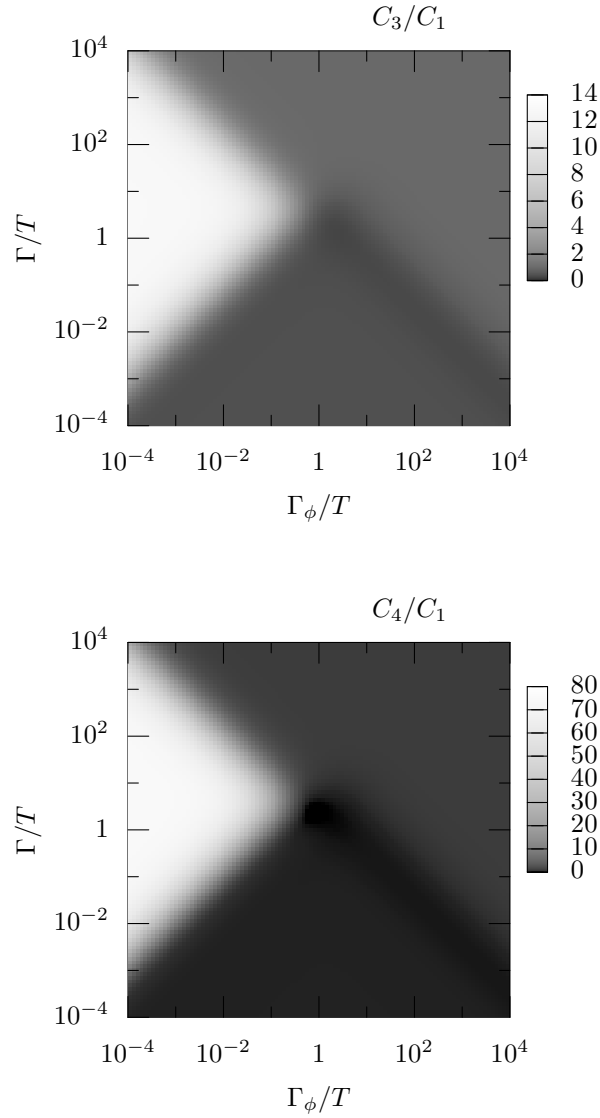


Figure 4.4.: “Generalized Fano factors” as a function of normalized decoherence rate  $\Gamma_\phi/T$  and normalized reservoir-dot tunnel rate  $\Gamma/T$ .  $C_3/C_1$ , plotted at the top, characterizes asymmetry (“skewness”).  $C_4/C_1$ , plotted at the bottom, characterizes kurtosis (“sharpness”). In the center,  $C_4/C_1$  reaches slightly negative ( $\simeq -0.02$ ) values. However, no qualitatively new features appear compared with the Fano factor  $C_2/C_1$  plotted in Fig. 4.3.

## 4. Solution and results

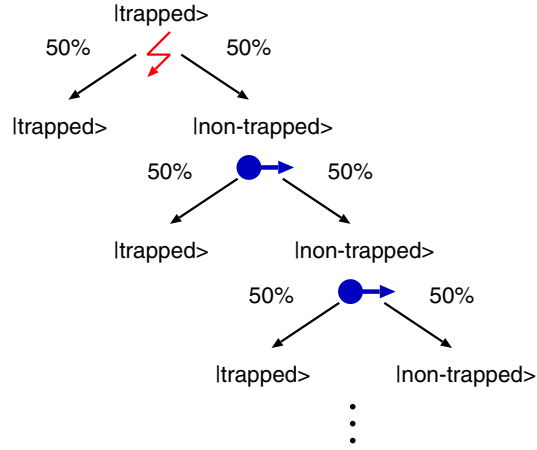


Figure 4.5.: Tunneling of electrons after a single decoherence event in the limit of weak decoherence.

## 4.2. Limits

### 4.2.1. Weak decoherence

For decoherence rate  $\Gamma_\phi \ll \Gamma, T$ , we have the limiting behavior

$$\langle I \rangle = e\Gamma_\phi + \mathcal{O}(\Gamma_\phi^2), \quad \alpha = 3 - \Gamma_\phi \left( \frac{17}{\Gamma} + \frac{\Gamma}{T^2} \right) + \mathcal{O}(\Gamma_\phi^2). \quad (4.10)$$

Hence one charge is transferred on average per decoherence event, but the Fano factor is three times the value for independent charge transfers.

There exists a simple physical explanation of this behavior. For zero decoherence the system becomes trapped in the state  $|e_2\rangle$ . If decoherence is weak, we expect the system to be *almost always* trapped. Indeed, we see from the limiting behavior of the stationary solution (4.6),

$$w_0 = \left[ \left( \frac{\Gamma}{8T^2} + \frac{1}{\Gamma} \right) \Gamma_\phi, 1 - \left( \frac{\Gamma}{8T^2} + \frac{5}{2\Gamma} \right) \Gamma_\phi, \frac{\Gamma_\phi}{\Gamma}, \frac{\Gamma_\phi}{2\Gamma}, \frac{\Gamma_\phi}{2\sqrt{2}\Gamma} \right]^T + \mathcal{O}(\Gamma_\phi^2), \quad (4.11)$$

that the system is trapped, up to a correction of order  $\Gamma_\phi$ .

We propose to think of the system being untrapped by “decoherence events”, which occur randomly at the rate  $\Gamma_\phi$  according to Poisson statistics. If  $\Gamma_\phi$  is sufficiently small, there is enough time for the system to decay into the trapped state between two subsequent events, so they can be viewed as independent. The super-Poissonian statistics appears because a single decoherence event can trigger the transfer of more than a single charge.

The probability of  $n$  electrons being transferred in total as a consequence of one decoherence event is

$$R^1(n) = \frac{1}{2^{n+1}}, \quad (4.12)$$

since a decoherence event projects the trapped state  $|e_2\rangle$  onto itself or onto  $|e_1\rangle$  with equal probabilities  $1/2$  and each electron subsequently entering the dots has a 50% chance of getting trapped in the state  $|e_2\rangle$  (see Fig. 4.5).

The number of electrons which have been transferred due to exactly  $k$  decoherence events has distribution  $R^k(n)$ , the  $(k-1)$ th convolution of  $R^1(n)$  with itself. We get (defining  $n_k = n - \sum_{i=1}^{k-1} n_i$ )

$$\begin{aligned} R^k(n) &= \sum_{n_1=0}^n \sum_{n_2=0}^{n_1} \cdots \sum_{n_{k-1}=0}^{n_{k-2}} \prod_{i=1}^k R^1(n_i) \\ &= \frac{1}{2^{n+k}} \sum_{n_1=0}^n \sum_{n_2=0}^{n_1} \cdots \sum_{n_{k-1}=0}^{n_{k-2}} 1 \\ &= \frac{1}{2^{n+k}} \binom{n+k-1}{n}. \end{aligned} \quad (4.13)$$

Note that  $\binom{n+k-1}{n} = \binom{n+k-1}{k-1}$  is the number of ways  $n$  electron transfers can be distributed among  $k$  decoherence events. By definition,

$$R^0(n) = \delta_{n,0} = \begin{cases} 1 & \text{for } n = 0 \\ 0 & \text{for } n > 0 \end{cases}, \quad (4.14)$$

being the distribution of the transferred charges after no decoherence events have occurred.

The decoherence events in a time  $t$  have a Poisson distribution,

$$P_{\text{Poisson}}(k) = e^{-t\Gamma_\phi} (t\Gamma_\phi)^k / k!. \quad (4.15)$$

Combining with Eq. (4.13), we find the probability that  $n$  electrons have been transferred during a time  $t$ ,

$$\begin{aligned} P(n) &= \sum_{k=0}^{\infty} P_{\text{Poisson}}(k) R^k(n) \\ &= \sum_{k=1}^{\infty} \frac{e^{-t\Gamma_\phi} (t\Gamma_\phi)^k}{2^{n+k} k!} \binom{n+k-1}{n} + e^{-t\Gamma_\phi} \delta_{n,0}. \end{aligned} \quad (4.16)$$

The corresponding cumulant generating function is

$$F(\chi) = t\Gamma_\phi - \frac{t\Gamma_\phi}{2 - e^{i\chi}}, \quad (4.17)$$

which gives rise to the cumulants

$$C_1 = t\Gamma_\phi, \quad C_2 = 3t\Gamma_\phi, \quad (4.18)$$

in agreement with Eq. (4.10).

#### 4. Solution and results

The probability distribution (4.17) has been found by Belzig in a different model [4]. As shown in that paper, this superposition of Poisson distributions with Fano factor 3 arises generically whenever there are two transport channels with very different transport rates (in our case slow transport via the trapped state  $|e_2\rangle$ , and fast transport via the untrapped state  $|e_1\rangle$ ).

##### 4.2.2. Weak dot-reservoir coupling

For decoherence rate  $\Gamma \ll \Gamma_\phi, T$ , we find

$$\langle I \rangle = \frac{2}{7}e\Gamma + \mathcal{O}(\Gamma^2), \quad \alpha = \frac{37}{49} - \left( \frac{18\Gamma_\phi}{343T^2} + \frac{36}{343\Gamma_\phi} \right) \Gamma + \mathcal{O}(\Gamma^2). \quad (4.19)$$

The stationary solution (4.6) is in this limit

$$w_0 = \begin{pmatrix} \frac{2}{7} + \left( \frac{3\Gamma_\phi}{98T^2} - \frac{4}{49\Gamma_\phi} \right) \Gamma \\ \frac{2}{7} + \left( \frac{3\Gamma_\phi}{98T^2} + \frac{10}{49\Gamma_\phi} \right) \Gamma \\ \frac{2}{7} - \left( \frac{2\Gamma_\phi}{49T^2} + \frac{4}{49\Gamma_\phi} \right) \Gamma \\ \frac{1}{7} - \left( \frac{\Gamma_\phi}{49T^2} + \frac{2}{49\Gamma_\phi} \right) \Gamma \\ \frac{\Gamma}{7\sqrt{2}T} \end{pmatrix} + \mathcal{O}(\Gamma^2), \quad (4.20)$$

showing that up to a correction of order  $\Gamma$ , the system stays in a mixed state, in which the three dots are equally populated with probabilities  $2/7$ . This is the consequence of the system being mixed by dot-dot-couplings and by decoherence at a rate much faster than the rate of entering and leaving the system.

In this limit, the three-dot system behaves like a single dot, connected to the left lead via a coupling  $2\Gamma$  (as there are two channels leading into the system), and to the right lead via a coupling  $\Gamma/3$  (as the electron is spread equally across the three dots). Compare Eq. (2.35).

##### 4.2.3. Strong decoherence

In the limit  $\Gamma_\phi \gg \Gamma, T$ , we get

$$\langle I \rangle = 2e \frac{\Gamma^2}{\Gamma_\phi} + \mathcal{O}\left(\frac{1}{\Gamma_\phi^2}\right), \quad \alpha = 1 - \frac{6\Gamma^2}{\Gamma\Gamma_\phi} + \mathcal{O}\left(\frac{1}{\Gamma_\phi^2}\right). \quad (4.21)$$

The stationary solution (4.6) becomes

$$w_0 = \left( \frac{1}{2} - \frac{3\Gamma^2}{2\Gamma\Gamma_\phi}, \frac{1}{2} - \frac{3\Gamma^2}{2\Gamma\Gamma_\phi}, \frac{2\Gamma^2}{\Gamma\Gamma_\phi}, \frac{\Gamma^2}{\Gamma\Gamma_\phi}, \frac{\Gamma}{\sqrt{2}\Gamma_\phi} \right)^T + \mathcal{O}\left(\frac{1}{\Gamma_\phi^2}\right). \quad (4.22)$$

We see that, up to corrections of order  $\Gamma_\phi^{-2}$ , the system resides in an incoherent superposition of states  $|e_1\rangle$  and  $|e_2\rangle$ , or (equivalently) states  $|A\rangle$  and  $|B\rangle$ .

The mechanism behind this behavior is the quantum Zeno effect (see App. C): Decoherence measures the electron's location at the very high rate  $\Gamma_\phi$ , continuously projecting the state of the system onto the basis states  $|A\rangle$ ,  $|B\rangle$ , and  $|C\rangle$ . This effectively weakens the tunnel couplings between the dots. As a consequence, the left dots are constantly filled, while the right dot is almost empty.

Occasionally, an electron will "escape" into the right dot and into the drain reservoir. This events occur independently leading to Poisson statistics, because a new electron will enter the left dots very quickly after the "escape". There is neither a queuing mechanism (as in the symmetrically coupled single dot, see Sec. 2.4) nor a memory of previous events (as in the limit of weak decoherence) to create correlations between electrons.

#### 4.2.4. Strong dot-reservoir coupling

Results for the limit  $\Gamma \gg \Gamma_\phi, T$ , also indicate Poisson statistics:

$$\langle I \rangle = 4e \frac{T^2}{\Gamma} + \mathcal{O}\left(\frac{1}{\Gamma^2}\right), \quad \alpha = 1 + \mathcal{O}\left(\frac{1}{\Gamma^2}\right). \quad (4.23)$$

The limiting behavior of the stationary solution (4.6),

$$w_0 = \left( \frac{1}{2} - \frac{2T^2}{\Gamma\Gamma_\phi}, \frac{1}{2} + \frac{2T^2}{\Gamma\Gamma_\phi}, 0, 0, \frac{\sqrt{2}T}{\Gamma} \right)^T + \mathcal{O}\left(\frac{1}{\Gamma^2}\right), \quad (4.24)$$

shows that the system stays, up to corrections of order  $\Gamma^{-2}$ , in an incoherent superposition of states  $|e_1\rangle$  and  $|e_2\rangle$ , or (equivalently) states  $|A\rangle$  and  $|B\rangle$ . This is easily comprehended, as the strong coupling between the source reservoir and the left dots keeps filling them up, while the strong coupling between the right dot and the drain reservoir depletes the right dot.

In this picture, however, it seems paradoxical that  $\langle I \rangle$  depends inversely on  $\Gamma$ . Why should dot-reservoir tunneling at a yet higher rate inhibit the current? Again quantum Zeno effect is the culprit: the right lead acts as a broadband detector constantly probing whether dot C is occupied or not. This effectively lowers the dot-dot couplings which are already the bottleneck of transport in this case.

The argument for the appearance of Poisson statistics is the same as for strong decoherence in Sec. 4.2.3.

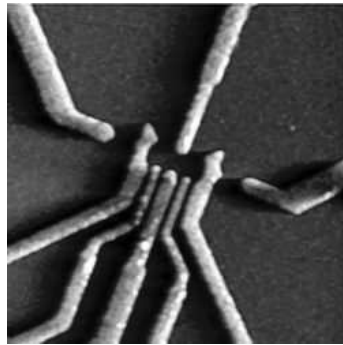
#### 4. *Solution and results*

## A. Quantum dots

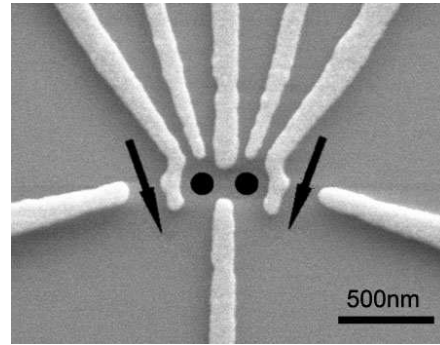
Quantum dots [16] are nanoelectronic devices which confine electrons or holes in all three dimensions. This results in a quantized energy spectrum earning quantum dots the nickname “artificial atoms”. It is today possible to confine a few or even single electrons in quantum dots [15]. First fabricated in the 1970s [23], quantum dots are now routinely manufactured lithographically on semiconducting substrates.

Typically, in a quantum dot charges are first confined in one dimension in a so-called heterostructure, which is composed of layers of dissimilar semiconductor material (often GaAs/AlGaAs). The 2-dimensional electron gas thus created is further electrostatically confined in the remaining two dimensions by metallic gates placed on top of the heterostructure. The shape of the gates and the voltage applied determine the electrostatic potential felt by the electron gas. Fig. A.1 displays two micrographs of double quantum dots. A system of three quantum dots, as described in Chap. 3, could be realized in a similar way.

## A. Quantum dots



(a) Atomic force microscope image of a double quantum dot. Reproduced with kind permission of Dr. L. M. K. Vandersypen, TU Delft.



(b) Scanning electron microscope image of a double quantum dot. The dots are indicated by filled circles, the quantum point contacts by arrows. Reproduced with kind permission of Dr. S. Ludwig, LMU München.

Figure A.1.: Micrographs of two pairs of tunnel-coupled quantum dots with quantum point contacts (QPCs) on both sides. The current through the QPCs is modulated by the state of the dots thus allowing to measure their state. The GaAs/AlGaAs heterostructure (dark background), which contains the two-dimensional electron gas, and the lithographically patterned gates (light foreground) are clearly visible.

## B. Lindblad master equation

In 1976, Lindblad presented [17] an differential equation describing the time evolution of an open quantum system, the *Lindblad master equation*. A quite exact derivation and further references can be found in the lecture notes by Preskill [22], and in the books by Nielsen and Chuang [21], and Le Bellac [3].

To derive the Lindblad equation, one considers the unitary evolution of the closed supersystem consisting of the system and its environment. One makes the Markov approximation that the environment is memory-less (This approximation is reasonable for a very big environment whose disturbance by the system can be neglected.) and traces-out the environment degrees of freedom. Finally, one arrives at an equation describing the non-unitary time evolution of the system's density matrix  $\rho$ :

$$\frac{d\rho}{dt} = -i[H, \rho(t)] + \sum_{\mu} \left( L_{\mu}\rho(t)L_{\mu}^{\dagger} - \frac{1}{2}L_{\mu}^{\dagger}L_{\mu}\rho(t) - \frac{1}{2}\rho(t)L_{\mu}^{\dagger}L_{\mu} \right), \quad (\text{B.1})$$

where  $H$  is the Hamiltonian of the system and  $L_{\mu}$  are non-hermitian *quantum jump operators* which describe the possible interactions of the system with the environment. A possible transition, induced by the environment at the rate  $\Gamma$ , for the system to jump from state  $|0\rangle$  to state  $|1\rangle$  is modelled by the jump operator

$$L_{0\rightarrow 1} = \sqrt{\Gamma}|1\rangle\langle 0|. \quad (\text{B.2})$$

Notice that in the absence of jump operators Eq. (B.1) becomes the quantum Liouville equation, the equation describing the time evolution of the density matrix of a closed system.

*B. Lindblad master equation*

## C. Quantum Zeno effect

Zeno of Elea, a Greek philosopher who lived during the fifth century BC, devised a set of famous paradoxes [11]. In one of his problems, Zeno claims that movement is not possible. He argues that because an object is precisely localized at a certain instant, it does not move at that instant. But time is just a collection of instants, he continues, and therefore the object is always at rest. In kinematics this “paradox” is resolved by infinitesimal calculus.

In 1977, Misra and Sudarshan proposed a quantum version of Zeno’s paradox [19] in which a quantum system is held in a certain state by measurements executed in quick succession. On the level of basic quantum mechanics this so called quantum Zeno effect is not paradoxal at all and can be understood as follows.

Consider a two level system

$$H = T|0\rangle\langle 1| + T|1\rangle\langle 0|, \quad T > 0, \quad (\text{C.1})$$

for example two tunnel-coupled quantum dots holding a single electron. Suppose we start out with the system in state  $|0\rangle$ . The probability to measure the system being in state  $|0\rangle$  after a short time  $\tau$  is

$$p(\tau) = |\langle 0|e^{-iH\tau}|0\rangle|^2 = \left| \langle 0| \left( \sum_{n=0}^{\infty} \frac{(-iH\tau)^n}{n!} \right) |0\rangle \right|^2 = \left| \sum_{m=0}^{\infty} \frac{(-T\tau)^{2m}}{(2m)!} \right|^2 \quad (\text{C.2})$$

$$= \cos^2(T\tau). \quad (\text{C.3})$$

Hence the probability to find the system in state  $|0\rangle$  after a time  $t$  during which we execute  $N$  regularly spaced measurements is  $\cos^{2N}(Tt/N)$ . As  $N$  approaches infinity,  $\cos^{2N}(Tt/N)$  approaches 1. If we perform the measurements sufficiently densely, the system always stays in state  $|0\rangle$ .

The question remains if it is possible to execute measurements sufficiently quickly for the Zeno effect to appear. An experimental demonstration was reported in 1990 by Itano [13]. Whether this experiment indeed displays the quantum Zeno effect remains a matter of intense debate [12].

The quantum Zeno effect can be also modelled with a Lindblad master equation (see App. B). Consider the same system as above. We model the repeated measurements with the quantum jump operator  $L = \sqrt{\Gamma}|0\rangle\langle 0|$ . The density matrix evolves according to

$$\begin{aligned} \frac{d\rho}{dt} &= -i[H, \rho(t)] + L\rho(t)L^\dagger - \frac{1}{2}L^\dagger L\rho(t) - \frac{1}{2}\rho(t)L^\dagger L \\ &= \begin{pmatrix} -2T\text{Im}(\rho_{01}) & iT(\rho_{00} - \rho_{11}) - \Gamma\rho_{01}/2 \\ iT(\rho_{11} - \rho_{00}) - \Gamma\rho_{10}/2 & 2T\text{Im}(\rho_{01}) \end{pmatrix}. \end{aligned} \quad (\text{C.4})$$

### *C. Quantum Zeno effect*

We see that tunneling between the states  $|0\rangle$  and  $|1\rangle$  is mediated by the imaginary part of the non-diagonal elements of  $\rho$ . But these decay at the rate  $\Gamma/2$  under the influence of repeated measurements  $L$ . By increasing  $\Gamma$ , a  $\rho$  which starts out as either  $|0\rangle\langle 0|$  or  $|1\rangle\langle 1|$  can be kept in that state for an arbitrary long time.

## Bibliography

- [1] D. A. Bagrets and Y. V. Nazarov, *Full counting statistics of charge transfer in coulomb blockade systems*, Physical Review B **67** (2003), 085316.
- [2] C. W. J. Beenakker and C. Schonberger, *Quantum shot noise*, Physics Today **56** (2003), 37, arXiv:cond-mat/0605025.
- [3] M. Le Bellac, *Quantum physics*, Cambridge University Press, 2006.
- [4] W. Belzig, *Full counting statistics of super-poissonian shot noise in multilevel quantum dots*, Physical Review B **71** (2005), 161301(R).
- [5] Y. M. Blanter and M. Buttiker, *Shot noise in mesoscopic conductors*, Physics Reports **336** (2000), 1, arXiv:cond-mat/9910158.
- [6] Tobias Brandes, *Coherent and collective quantum optical effects in mesoscopic systems*, Physics Reports **408** (2005), 315.
- [7] M. J. M. de Jong and C. W. J. Beenakker, *Shot noise in mesoscopic systems*, Mesoscopic Electron Transport **345** (1997), 225, arXiv:cond-mat/9611140.
- [8] S. A. Gurvitz, *Rate equations for quantum transport in multi-dot systems*, Physical Review B **57** (1998), 6602.
- [9] S. Gustavsson, R. Leturcq, B. Simovic, R. Schleser, T. Ihn, P. Studerus, K. Ensslin, D. C. Driscoll, and A. C. Gossard, *Counting statistics of single-electron transport in a quantum dot*, Physical Review Letters **96** (2006), 076605.
- [10] S. Gustavsson, R. Leturcq, B. Simovic, R. Schleser, P. Studerus, T. Ihn, K. Ensslin, D. C. Driscoll, and A. C. Gossard, *Counting statistics and super-poissonian noise in a quantum dot*, 2006, arXiv:cond-mat/0605365, p. 195305.
- [11] N. Huggett, *Zeno's paradoxes*, Stanford Encyclopedia of Philosophy, 2004, <http://plato.stanford.edu/entries/paradox-zeno/>.
- [12] W. M. Itano, *Perspectives on the quantum zeno paradox*, 2006, arXiv:quant-ph/0612187.
- [13] W. M. Itano, D. J. Heinzen, J. J. Bollinger, and D. J. Wineland, *Quantum zeno effect*, Physical Review A **41** (1990), 2295.

## Bibliography

- [14] G. Kiesslich, P. Samuelsson, A. Wacker, and E. Schoell, *Counting statistics and decoherence in coupled quantum dots*, Physical Review B **73** (2006), 033312, arXiv:cond-mat/0507403.
- [15] L. P. Kouwenhoven, D. G. Austing, and S. Tarucha, *Few-electron quantum dots*, Reports on Progress in Physics **6** (2001), no. 64, 701.
- [16] L. P. Kouwenhoven and C. M. Marcus, *Quantum dots*, Physics World **11** (1998), no. 6, 35.
- [17] G. Lindblad, *On the generators of quantum dynamical semigroups*, Communications in Mathematical Physics **48** (1976), 119.
- [18] B. Michaelis, C. Emary, and C. W. J. Beenakker, *All-electronic coherent population trapping in quantum dots*, Europhysics Letters **73** (2006), 677.
- [19] B. Misra and E. C. G. Sudarshan, *The zeno's paradox in quantum theory*, Journal of Mathematical Physics **18** (1977), 756.
- [20] Y. V. Nazarov, *Quantum interference, tunnel junctions and resonant tunneling interferometer*, Physica B **189** (1993), 57.
- [21] M. A. Nielsen and I. L. Chuang, *Quantum computation and quantum information*, Cambridge University Press, 2000.
- [22] J. Preskill, *Quantum information and computation*, Lecture Notes for Physics 229, 1998, <http://www.theory.caltech.edu/people/preskill/ph229/>.
- [23] M. A. Reed, J. N. Randall, R. J. Aggarwal, R. J. Matyi, T. M. Moore, and A. E. Wetsel, *Observation of discrete electronic states in a zero-dimensional semiconductor nanostructure*, Physical Review Letters **60** (1988), 535.
- [24] Jens Siewert and Tobias Brandes, *Applications of adiabatic passage in solid-state devices*, Adv. Solid State Phys. **44** (2004), 181.